THE JOURNAL OF BIOLOGICAL CHEMISTRY
Vol. 280, No. 1, Issue of January 7, pp. 538–547, 2005
Printed in U.S.A.

Identification of a Region of Fast Skeletal Troponin T Required for Stabilization of the Coiled-coil Formation with Troponin I*

Received for publication, August 19, 2004, and in revised form, October 25, 2004
Published, JBC Papers in Press, October 26, 2004, DOI 10.1074/jbc.M409537200

Subhradip Mukhopadhyay‡§, Knut Langsetmo¶, Walter F. Stafford III¶, Gillian D. Henry‖, James D. Baleja‖, and Satyapriya Sarkar‡‡‡**

*From the ‡Program in Cell, Molecular and Developmental Biology, Sackler School of Graduate Biomedical Sciences, and the Departments of **Anatomy and Cell Biology and ‖Biochemistry, Tufts University School of Medicine, Boston, Massachusetts 02111, the §Department of Biochemistry, University College of Science, University of Calcutta, Calcutta 700019, India, and the ¶Boston Biomedical Research Institute, Watertown, Massachusetts 02472*

We have previously identified evolutionarily conserved heptad hydrophobic repeat (HR) domains in all isoprotein members of troponin T (TnT) and troponin I (TnI), two subunits of the Ca^{2+}-regulatory troponin complex. Our suggestion that the HR domains are involved in the formation of a coiled-coil heterodimer of TnT and TnI has been recently confirmed by the crystal structure of the core domain of the human cardiac troponin complex. Here we studied a series of recombinant deletion mutants of the fast skeletal TnT to determine the minimal sequence required for stable coiled-coil formation with the HR domain of the fast skeletal TnI. Using circular dichroism spectroscopy, we measured the α helical content of the coiled-coil formed by the various TnT peptides with TnI HR domain. Sedimentation equilibrium experiments confirmed that the individual peptides of TnT were monomeric but formed heterodimers when mixed with HR domain of TnI. Isothermal titration calorimetry was then used to directly measure the affinity of the TnT peptides for the TnI HR domain. Surprisingly we found that the HR regions alone of the fast skeletal TnT and TnI, as defined earlier, were insufficient to form a coiled-coil. Furthermore we showed that an additional 14 amino acid residues N-terminal to the conserved HR region (TnT residues 165–178) are essential for the stable coiled-coil formation. We discuss the implication of our finding in the fast skeletal troponin isoform in the light of the crystal structure of the cardiac isoform.

Vertebrate striated muscle contraction is regulated by Ca^{2+}, and the proteins that mediate this regulation in the contractile muscle are tropomyosin (Tm)[1] and troponin (Tn) (for reviews, see Refs. 1–6). The Tm-Tn complex binds polymerized actin to form the regulated thin filament. Actin, Tm, and Tn are present in the thin filament in a ratio of 7:1:1 (2). Tm is an α helical coiled-coil protein and interacts with another Tm molecule in a head-to-tail manner to form a strand that lies in the groove of the polymerized actin filament (2, 3). The Tn complex is composed of three structurally and functionally different proteins: troponin C (TnC), which binds to Ca^{2+}; troponin I (TnI), which binds to actin; and troponin T (TnT), which binds to Tm. In the relaxed muscle, TnI inhibits the ATPase activity of actomyosin by binding to actin and blocking the actin-myosin interaction (1, 4–6). In the excited muscle, depolarization of muscle membrane releases Ca^{2+} in the sarcoplasm, and the binding of this Ca^{2+} to TnC leads to a conformational change in TnC. This initiates muscle contraction through a process of "information transfer." Subsequent steps involve multiprotein interactions and conformational changes in the thin filament leading to the contraction of muscle. The information transfer during muscle contraction presumably follows the order: TnC → TnI → TnT → Tm → actin (1, 4–6).

All of the subunits of the Tn complex participate in binary and ternary interactions, and these play a critical role in the Ca^{2+} regulation of the muscle contraction. The natures of these interactions as well as the factors that influence them are key for understanding the contraction mechanism (1, 4–6). The involvement of TnT is particularly important in the regulatory system as TnT interacts with TnI, TnC, Tm, and actin (7). TnT anchors the whole Tn complex to the thin filament by interacting with the Tm head-to-tail overlapping region and thus plays a major structural role (3, 4, 7). Another function of TnT is to increase the cooperativity of the actin-Tm interaction. It is also required for the allosteric signal transduction in sensitizing the actin-activated myosin ATPase to the concentration of Ca^{2+} (8–10).

Studies reported in the literature for mapping the regions of TnT involved in intersubunit interactions and important for its biological activities have used wild type or mutant TnT proteins, either native or recombinant (7, 11–15). Fast skeletal TnT (fsTnT) can be cleaved by proteolytic digestion into two halves: TnT1 (residues 1–157) and TnT2 (residues 158–258) (7). Interestingly most of the biological activities and the sites of interactions of TnT with other thin filament proteins are located on these two fragments separately (7, 8, 16). The TnT1 fragment is mainly involved in the interaction with Tm, whereas the TnT2 fragment, which is located in the regulatory "globular" head of the Tn complex, is involved in the interac-

* This work was supported by National Institutes of Health Grants P01-HD 23681 and R01HL39374 (to S. S.) and GM 067985 (to J. D. B.), National Science Foundation Grant BIR-9513060 (to W. F. S.), and grants from the American Heart Association and Tufts University School of Veterinary Medicine (to S. S.). The costs of publication of this article were defrayed in part by the payment of page charges. This article must therefore be hereby marked "*advertisement*" in accordance with 18 U.S.C. Section 1734 solely to indicate this fact.

‡‡ To whom correspondence should be addressed: Dept. of Anatomy and Cellular Biology, Tufts University School of Medicine, M&V 519, 136 Harrison Ave., Boston, MA 02111. Tel.: 617-636-2931; Fax: 617-636-6536; E-mail: satyapriya.sarkar@tufts.edu.

[1] The abbreviations used are: Tm, tropomyosin; Tn, troponin; TnT, troponin T; TnI, troponin I; TnC, troponin C; fsTnT, fast skeletal troponin T; fsTnI, fast skeletal troponin I; cTnT, cardiac TnT; HR, heptad hydrophobic repeat; TnT HR, peptide corresponding to the HR region of the fast skeletal troponin T; TnI HR, peptide corresponding to the HR region of the fast skeletal troponin I; TnT1, N-terminal proteolytic fragment of TnT; TnT2, C-terminal proteolytic fragment of TnT; ITC, isothermal titration calorimetry; βME, β-mercaptoethanol.

tions with TnC and TnI (7). TnT residues 235–250 have been suggested to interact with TnC (7, 17), and residues 178–250 have been implicated as the TnI interaction region (7, 12). This latter region contains an evolutionarily conserved region (residues 179–241), previously identified by us, with heptad hydrophobic repeats (HRs), known for their ability to form coiled-coil structures (18, 19). A similar region, presumably derived from a common ancestor gene, is also present in TnI (residues 58–114) (20). Based on point and deletion mutagenesis of the HR region of fsTnT and loss of interaction with fsTnI using the yeast two-hybrid assay, it was suggested that these regions of TnT and TnI form a heterodimeric α helical coiled-coil (18). A recent report of the crystal structure of the core domain of the human cardiac Tn complex, comprising cardiac TnC and the C-terminal fragments of cardiac TnI and TnT, confirmed these interactions (21). In the crystal structure, residues 226–271 of cTnT makes an α helical coiled-coil with residues 90–135 of cTnI.

The importance of the heterodimeric coiled-coil region as a major structural domain in the Tn complex is evident from the crystal structure of the cardiac Tn core complex. But an understanding of the details, particularly how this region in the fast skeletal isoform plays a role in the binary interaction with TnI, is limited due to lack of any crystal structure of the fast skeletal isoform. To gain further insight into the TnT-TnI interaction, in the present study we examined the parameters of the heterodimeric coiled-coil formation of the fast skeletal Tn isoform using recombinant peptides made from TnT and TnI. We constructed fsTnT fragments encompassing the region between amino acid residues 158–258 and examined their ability to form a coiled-coil with TnI HR. We showed that whereas a TnT fragment containing only the HR region forms a weak coiled-coil with the HR region of TnI, a TnT fragment containing the additional amino acid residues 165–178, N-terminal to the HR region, forms a much stronger coiled-coil. It was concluded that a region outside the HR domain of fsTnT is critically required for the stability of this interaction.

EXPERIMENTAL PROCEDURES

Materials—Common reagents and buffer components were purchased from Sigma unless mentioned otherwise. PCR reagents were from Roche Applied Science, and oligonucleotides were purchased from Integrated DNA Technologies (Coralville, IA). Restriction enzymes were purchased from New England Biolabs (Beverly, MA). The DNA purification kit, gel elution kit, and nickel-nitrilotriacetic acid-agarose used for protein purification were purchased from Qiagen (Valencia, CA).

Constructions of Plasmids for Expression of Recombinant Peptides—Oligonucleotides for the construction of the TnT2 and its deletion mutants were designed based on the human fast skeletal troponin T β cDNA sequence (22) that was cloned into the pET-28a expression vector. Primers were designed so that the 5′ primers contained an NdeI restriction site and the 3′ primers contained an XhoI restriction site. Primers 1 (5′-ACTACAGCCATATGCTGGCCAAGGC-3′) and 2 (5′-CTGCTCGAGCTACTTCCAGCGCC-3′) were used to PCR-amplify the TnT2 region. Primers 3 (5′-TGAAGAAGCATATGCTGGCTGAGAGAC-3′) and 4 (5′-AGCCTCGAGTTAGTGCTTCTGGGCCTG-3′) were used for amplifying the HR region. Primer pairs 1/4 and 2/3 were used for amplifying the region corresponding to the TnT-(158–241) and TnT-(179–258), respectively. Primer 5 (5′-AGGCTGACCATATGAGAGGCAAGAAG-3′) and primer 4 were used for amplification of the TnT-(165–241) region. In a similar way, primer 6 (5′-AGAAGCAGCATATGCGAGAGATGAAG-3′) and primer 4 were used for amplifying the region corresponding to TnT-(172–241). Primer 5 was used with primer 7 (5′-GGCCTCGAGTTAGCGGCTCCTGAGCG-3′) and primer 8 (5′-GATCTCGAGTTAGTCATATTTCTGGCG-3′) for amplifications of TnT-(165–234) and TnT-(165–227) regions, respectively. After the PCRs, the products were digested with NdeI and XhoI and subsequently cloned into pET-28a expression vector, previously digested with the same NdeI and XhoI restriction enzymes.

A rabbit fast skeletal TnI cDNA (23) was subcloned into pET-28a. A fragment corresponding to amino acids 57–112 was PCR-amplified using primers 9 (5′-TCCCCGGCCATATGGCCGAGGTGC-3′) and 10 (5′-CATCTCGAGCTACCGCAGCGGGGGCCTC-3′). After the PCR, the products were digested with NdeI and XhoI and cloned into pET-28a in the same way as above. All the subcloned constructs were verified by DNA sequencing.

Expression and Purification of Recombinant Peptides—For production of the recombinant peptides, constructs were transformed into *Escherichia coli* BL21 (DE3) pLysS cells and were grown in a LB medium containing 50 μg/ml kanamycin and chloramphenicol overnight at 37 °C. One liter of LB medium containing the same antibiotics was then inoculated with 20 ml of the overnight culture, and the cells were grown at 37 °C until the OD reached 0.5, and then 1 mM isopropyl β-D-thiogalactopyranoside was added. To facilitate selective production of plasmid-encoded proteins, rifampicin was added at 50 μg/ml 30 min after the addition of isopropyl β-D-thiogalactopyranoside. Cells were then grown for 5 h, harvested by centrifugation, and stored at −80 °C.

Bacterial cells containing the various His-tagged peptides were lysed using the freeze-thaw technique. The peptides were recovered from the inclusion bodies by solubilization in buffer B (20 mM Tris-HCl, pH 8.0, and 8 M urea) and centrifuged at 10,000 × *g* for 20 min, and the supernatant was collected. 10 ml of 50% (w/v) nickel-nitrilotriacetic acid-agarose, previously equilibrated in the same buffer, was then added to the supernatant and incubated at room temperature for 2 h with rotation. The material was then transferred to a column and washed sequentially with buffer B, then with buffer B containing 10 mM imidazole, and with buffer B containing 20 mM imidazole. His-tagged peptides were eluted from the column by a wash with buffer B containing 250 mM imidazole.

The eluted peptides in denaturing buffer were then subjected to renaturation by step dialysis. Typically 15 ml of the peptide solution was packed into a Spectrapore dialysis bag and dialyzed for 10 h stepwise in three buffers containing 20 mM Tris-HCl, pH 7.5, 300 mM NaCl, and 4, 2, and 0 M urea, respectively. For the separation of the His tag from the peptides, when necessary, the Biotinylated Thrombin kit (Novagen) was used following the manufacturer's protocol. The cleaved His tag was separated from the solution by passing the reaction mixture through a DG 10 column (Bio-Rad).

Circular Dichroism Spectroscopy—CD spectroscopic measurements were performed on a Jasco 810 spectropolarimeter (Jasco, Easton, MD) fitted with a Peltier temperature controller. The instrument was calibrated with an aqueous solution of *d*-10-(+)-camphor sulfonic acid at 290.5 nm. Samples were extensively dialyzed in a 10 mM Tris-HCl, 300 mM NaF, 0.5 mM dithiothreitol, pH 7.5 buffer before the measurements. All spectra measurements were recorded at 5 °C. Data were recorded at 0.2-nm intervals from 270 to 190 nm at a scanning speed of 2 nm/min. A 1-mm path length quartz cell was used for the measurements. For all runs, the base line was corrected by subtracting a spectrum of the buffer from the spectrum of the protein. Secondary structure analysis was performed using the Selcon2 program (24).

For temperature denaturation studies, ellipticity was recorded at 222 nm as the temperature was increased from 0 to 75 °C at a rate of 2 °C/min (25). The T_m values were extracted by fitting the thermal denaturation data to Equation 1,

$$\theta = f_M\theta_M + (1 - f_M)\theta_D \qquad \text{(Eq. 1)}$$

where f_M is the fraction of monomer and θ_M and θ_D are the ellipticities of the monomer and dimer, respectively. The natural temperature dependence of the base-line slope was included by defining θ_M and $\theta_D = \theta_{(M\text{ or }D)0\text{ K}} + mT$, *i.e.* the value at 0 K plus a temperature dependence, m. f_M for a bimolecular dissociation is obtained from $K_d = [M]^2/[D] = 2f_M{}^2[P]/(1 - f_M)$ where $[P]$ is the total molar protein concentration. Rearranging the above equation gives Equation 2,

$$f_M = \frac{-K_d + \sqrt{K_d{}^2 + 8[P]K_d}}{4[P]} \qquad \text{(Eq. 2)}$$

K_d is related to T_m by substituting the integrated van't Hoff Equation 3 into Equation 2,

$$K_d = [P]\exp\left[\frac{\Delta H_{vH}}{R}\left(\frac{1}{T_m} - \frac{1}{T}\right)\right] \qquad \text{(Eq. 3)}$$

Equation 3 is valid if the difference between the heat capacities of the dimer and monomer (ΔC_p) is small. Fitted parameters were $\theta_{D0\text{ K}}$, $\theta_{M0\text{ K}}$, ΔH_{vH}, T_m, and m (26). The T_m values were checked by differentiating the data with respect to temperature and fitting it to the equation after application of a three-point smoothing window,

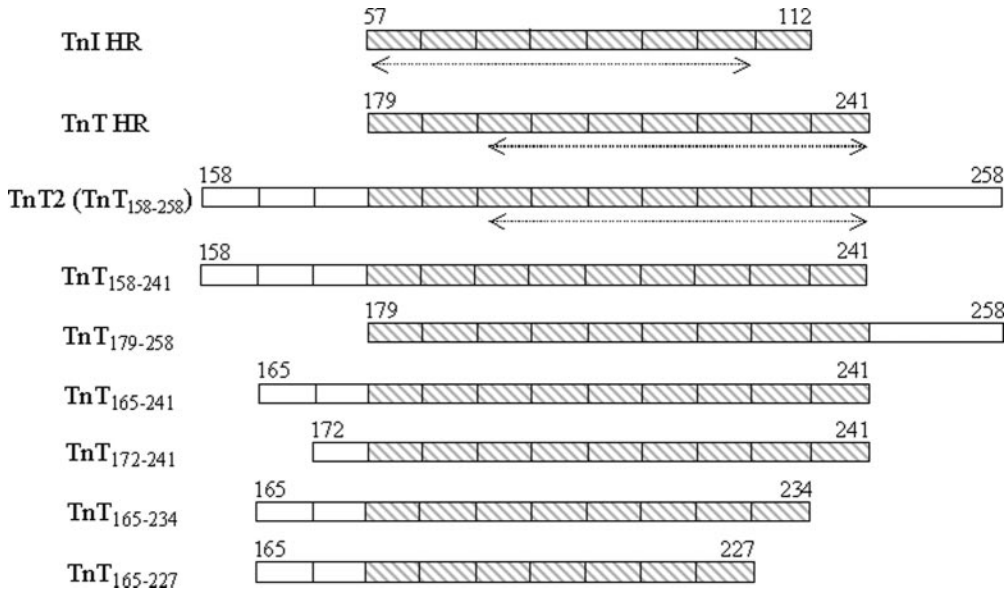

FIG. 1. **Scheme of the fast skeletal TnI and TnT fragments used in this study.** The amino acid numbers corresponding to the fast skeletal TnI and TnT are indicated *above* each molecule. The *positions* of the *arrows* indicate the amino acid residues that correspond to the regions of the cardiac TnI and TnT involved in the coiled-coil interaction. The evolutionarily conserved HR region present in both fast skeletal TnI and TnT is shown *shaded*. *Boxes* represent heptads, and *clear boxes* indicate the imperfect heptads in the N-terminus of TnT2.

$$d\theta/dT = Af_M(1 - f_M)T^2 \quad \text{(Eq. 4)}$$

where A is a scaling factor (27). This determines the point of inflection and is effective even when the thermal denaturation curves are incomplete. The T_m values reported are the average of two independent experiments, and the T_m values did not differ by more than 1 °C between the experiments.

Sedimentation Equilibrium Analysis—Sedimentation equilibrium ultracentrifugation was performed on a Beckman Coulter Optima X-LA model analytical ultracentrifuge using an eight-hole An-50Ti rotor. Samples were extensively dialyzed against a 10 mM Tris-HCl, 300 mM NaCl, 1 mM βME, pH 7.5 buffer, and centrifugation runs were performed in the same buffer. All experiments were performed at 5 °C at various speeds between 25,000 and 50,000 rpm. Double sector cells were filled with 250 μl of samples giving a column height of ~5 mm, and the data were recorded at 230 nm with a radial increment of 0.001 cm with 16 replicates. Scans were taken every 2 h during the approach of equilibrium. The attainment of equilibrium was verified using the WinMatch program. Data analysis was carried out with the equilibrium data fitter, which is a part of the program SEDANAL (28), using the non-linear least square method to fit globally to multiple data sets. The goodness of fit was determined by a minimum root mean square deviation comparable to the noise on the data and by randomly varying residuals. The partial specific volume of each peptide was calculated using the program SEDNTERP from the amino acid composition, and the solvent density was calculated using known values from physical tables also using SEDNTERP.

Isothermal Titration Calorimetry (ITC)—ITC experiments were performed using a VPITC calorimeter (Microcal Inc., Northampton, MA). Samples were dialyzed overnight at 4 °C in a 10 mM Tris-HCl, 300 NaCl, 1 mM βME, pH 7.5 buffer before the experiments. All experiments were performed at 5 °C. The sample cell was filled with a ~10 μM solution of TnI HR (volume, 1.4 ml), and the TnT fragments (10 times more concentrated) were titrated into the cell from the 300-μl syringe while stirring at 300 rpm. A typical experiment consisted of 28 successive automatic injections of 10 μl each with 180-s equilibration time between the injections. The first injection consisted of 2 μl and was ignored in the final data analysis. The heat change for the dilution of the ligand injections was measured by injecting the TnT2 fragments into the buffer under identical conditions and was subtracted from the measured heat change of ligand binding to protein. Data analysis was performed using the least square method with the Origin-based software provided by the manufacturer to determine the equilibrium binding constant (K_A), the enthalpy of the complex formation (ΔH), and the entropy (ΔS) of the reaction. All the reported thermodynamic parameters were calculated by averaging parameters obtained from at least two independent experiments, and the range of their values are also indicated.

Modeling of the Coiled-coil Domain—A model for the HR region of the fast skeletal TnI/TnI heterodimer was created from the x-ray crystal structure of the cardiac Tn core domain complex (21). Manual alignment of the sequences gave 57% identity in TnI and 62% identity in TnT. Residues 165–168 of fsTnT were given extended conformations because there was no electron density in the crystal structure for the corresponding residues of cTnT. Where needed, side chains were converted from those of cTnI/TnT to fsTnI/TnI using the Biopolymer module of InsightII (Accelrys Inc., San Diego, CA). Graphical representation was made using InsightII.

RESULTS

Design of the Peptides—Recombinant peptides corresponding to residues 179–241 in fsTnT and residues 57–112 in fsTnI were made to examine the hypothesis that the conserved HR domains are involved in coiled-coil formation (18). The peptides used to define the region of fsTnT involved in the formation of a stable TnT-TnI heterodimer are schematically represented in Fig. 1. Residues 193–238 of fsTnT HR and residues 58–103 of fsTnI HR correspond to the amino acid residues 226–271 and 90–135 of the cardiac TnT and TnI isoform, respectively, which are observed to form a heterodimeric coiled-coil in the crystal structure of the human cardiac troponin core complex (21). To determine whether these skeletal Tn residues were sufficient for coiled-coil formation, we began with TnT2 (amino acid residues 158–258) and examined various deletion mutants. TnT-(158–241) and TnT-(179–258) were made to determine the effect of additional amino acid residues at the C-terminal and N-terminal ends of the HR region, respectively. The TnT2 sequence contains three imperfect heptads between residues 158 and 178. TnT-(165–241) and TnT-(172–241) containing deletions of these imperfect heptads were designed. Also two C-terminal deletion mutants TnT-(165–234) and TnT-(165–227), containing deletions of one and two heptads, respectively, inside the HR region of TnT, were made to determine their role in the coiled-coil interaction. Unlike TnT, TnI does not contain additional heptad repeats outside the conserved HR domain, and therefore only the TnI HR peptide was used for studying the coiled-coil interaction with all the TnT2 fragments.

Secondary Structural Analysis by Circular Dichroism Spectroscopy—Since coiled-coil formation is dependent on the α helical characteristics of the interacting peptides, CD spectro-

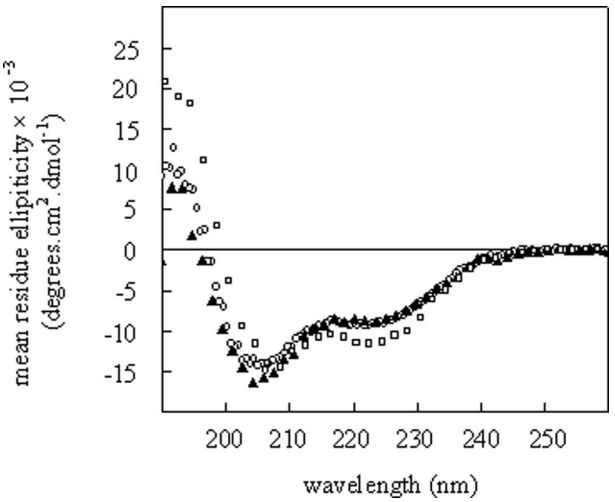

FIG. 2. **CD spectra of TnI HR (▲), TnT HR (□), and TnT2 (○).** Spectra were recorded at 5 °C in 10 mM Tris-Cl, pH 7.5, 300 mM NaF, and 1 mM dithiothreitol buffer. Concentrations of the peptides were 15 μM.

scopic analysis was used to determine the secondary structural properties of the peptides. The CD spectra of TnT HR, TnT2, and TnI HR are illustrated in Fig. 2. The TnT HR spectrum showed negative ellipticities around 222 and 208 nm, characteristic of proteins with helical content but also containing other secondary structures. The TnT2 spectrum also showed similar characteristics, although the amount of α helicity was slightly lower. The TnI HR spectrum, on the other hand, showed a broad minimum around 205 nm and lacked a well defined minimum around 222 nm. Secondary structure estimates are summarized in Table I.

As compared with the sum of the spectra of the individual peptides, the mean residue ellipticity value at 222 nm for the equimolar mixture of TnT HR and TnI HR increased considerably, and the spectra showed a shift toward both 208 and 222 nm minima characteristic of typical α helices (Fig. 3*A* and Table I). The increase in the α helix content to 45% (from 35% for the average of the individual peptides) is interpreted as the direct result of interaction between the helices and stabilization of the structure. The ratio of ellipticities θ_{222}:θ_{208} has been proposed to be diagnostic of coiled-coil formation. This ratio is 1.02–1.03 for a stable coiled-coil (25, 29–31). Although the HR regions of cardiac TnT and TnI form a coiled-coil (21), surprisingly the θ_{222}:θ_{208} ratio of 0.82 for the mixtures of fast skeletal HR domains indicated no coiled-coil formation, suggesting that the HR regions of TnT and TnI alone were insufficient for coiled-coil interaction.

In contrast to the TnT HR/TnI HR mixture, the CD spectrum of an equimolar mixture of TnT2 and TnI HR showed high helical content (Fig. 3*A* and Table I). The θ_{222}:θ_{208} ratio was 0.96, close to the ratio expected for a stable coiled-coil. TnT2 alone did not show high α helical characteristics (Fig. 2), suggesting that the increased helical content of the TnT2/TnI HR mixture was due to the stabilization by TnT2. This observation raised the possibility that the presence of additional amino acids in TnT2, residues 158–178 at the N-terminal and residues 242–258 at the C-terminal end of the HR region, may contribute to the stabilization of the coiled-coil interaction.

To determine whether the amino acid residues at the N-terminal or C-terminal or both were responsible for stabilization, we examined CD spectra of equimolar mixtures of TnT-(158–241)/TnI HR and TnT-(179–258)/TnI HR (Fig. 3*B*). As clearly evident, the TnT-(158–241)/TnI HR mixture showed helical properties identical to that of the TnT2/TnI HR peptide mixture with an α helical content of 61% and a θ_{222}:θ_{208} ratio of 0.96 (Table I), indicating that amino acid residues 158–178 were sufficient to have the same effect as TnT2. On the other hand, the TnT-(179–258)/TnI HR mixture resembled the structural characteristics of the TnT HR/TnI HR mixture (Fig. 3*B*), having a similar α helical content of 41% and θ_{222}:θ_{208} ratio of 0.78 (Table I). This indicated that the presence of C-terminal amino acid residues 242–258 did not have helix stabilizing capability compared with TnT HR.

Since the helix stabilizing capacity was limited to the N-terminal amino acid residues 158–178 of the TnT2 and this region contains three imperfect heptads, CD spectra were analyzed for TnT-(165–241) and TnT-(172–241) to determine the contribution of each heptad. Comparison of the spectra of TnT-(165–241)/TnI HR and TnT-(172–241)/TnI HR equimolar peptide mixtures indicated that both of them were similar in helical properties to the TnT-(158–241)/TnI HR mixture (Fig. 3*C*). The θ_{222}:θ_{208} ratios were 0.98 and 0.96, also similar to that of 0.96 for the TnT-(158–241)/TnI HR mixture. These suggested that amino acid residues 158–171 were not necessary for stabilization, whereas residues 172–178 were absolutely required.

To determine whether the C-terminal heptads inside the HR region of TnT were required for the stable coiled-coil formation, TnT-(165–234)/TnI HR and TnT-(165–227)/TnI HR equimolar mixtures were examined. The TnT-(165–234)/TnI HR mixture had similar helical properties to the TnT HR/TnI HR mixture (Fig. 3*D* and Table I). In contrast, the TnT-(165–227)/TnI HR mixture showed very poor α helical properties (Fig. 3*D*). θ_{222}:θ_{208} ratios were 0.82 and 0.72 for TnT-(165–234)/TnI HR and TnT-(165–227)/TnI HR mixtures, respectively, indicating no coiled-coil formation by both TnT-(165–234) and TnT-(165–227). This showed that the heptads inside the HR domain at the C-terminal were required for the stable coiled-coil interaction.

The relative stability of the coiled-coils formed by peptide mixtures of TnT2 fragments and TnI HR were determined by thermal denaturation. The temperature denaturation curves of the peptide mixtures of TnT2, TnT-(158–241), TnT-(179–258), and TnT HR each with TnI HR are shown in Fig. 4*A*. The TnT HR/TnI HR mixture had a T_m of 14 °C. In contrast, the TnT2/TnI HR mixture showed a well defined two-state denaturation profile and had a T_m of 24 °C. The ~10 °C difference in the melting temperature demonstrates the greater stability of the TnT2/TnI HR mixture. For TnT-(158–241)/TnI HR and TnT-(179–258)/TnI HR mixtures the T_m values were 23 and 14 °C respectively, clearly indicating the stability of the TnT-(158–241)/TnI mixture compared with the TnT-(179–258)/TnI HR mixture.

Melting curves of the peptide mixtures of TnT-(165–241), TnT-(172–241), and TnT-(165–234) with TnI HR are shown in Fig. 4*B*. TnT-(165–241)/TnI HR had a T_m (24 °C) similar to that of both TnT2/TnI HR and TnT-(158–241)/TnI HR mixtures. On the other hand the TnT-(172–241)/TnI HR mixture had a T_m of 21 °C, slightly lower than that of the TnT-(158–241)/TnI HR mixture, indicating that the presence of amino acid residues 165–171 was able to contribute additional stability to the complex. The TnT-(165–234)/TnI HR mixture had a T_m of 11 °C, even lower than that of TnT HR/TnI HR, showing that the C-terminal heptad inside the HR region was required for stable interaction. Results of the experiments are summarized in Table I.

Analytical Ultracentrifugation—We used sedimentation equilibrium to determine whether the CD spectra recorded for the individual peptides were due to monomeric or multimeric forms. Since it is known that TnI and TnT may aggregate at high concentration, it was most important to determine the

TABLE I
Secondary structural properties and stability of the peptides and their mixtures

Species name	α helix	β sheet	Other	Total[a]	θ_{222}:θ_{208}[b]	T_m[c]
	%	%	%	%		°C
TnI HR	32	16	52	100	ND[d]	ND
TnT HR	38	10	52	100	ND	ND
TnT2	30	14	56	100	ND	ND
TnT-(158–241)	32	11	55	98	ND	ND
TnT-(179–258)	30	15	55	100	ND	ND
TnT-(165–241)	30	13	54	97	ND	ND
TnT-(172–241)	30	14	54	100	ND	ND
TnT HR/TnI HR	45	3	52	100	0.82	14
TnT2 / TnI HR	60	5	32	97	0.96	24
TnT-(158–241)/TnIHR	61	7	32	100	0.94	23
TnT-(179–258) / TnI HR	41	4	44	99	0.78	14
TnT-(165–241)/TnI HR	59	6	35	100	0.98	24
TnT-(172–241)/TnI HR	58	5	25	97	0.96	21
TnT-(165–234)/TnI HR	43	5	52	100	0.82	11
TnT-(165–227)/TnI HR	33	12.5	54.5	100	0.72	ND

[a] Secondary structural content was determined using the Selcon2 program.
[b] θ_{222}:θ_{208} value is an indicator of the coiled-coil state of the interacting peptides. Because they were very less α helical and do not form any dimer, values for the individual peptides were not determined as indicated by ND.
[c] The T_m value was determined by fitting the temperature denaturation curve to Equation 1 as described under "Experimental Procedures." Determination of the point of inflection using Equation 4 yielded values 1 °C higher. T_m values represented here are the average of two independent measurements, and the difference in values was less than 1°C between measurements. Because of the extremely low α helicity, the T_m was not determined for the individual peptides and the TnT-(165–227)/TnI HR mixture as indicated by ND.
[d] ND, not determined.

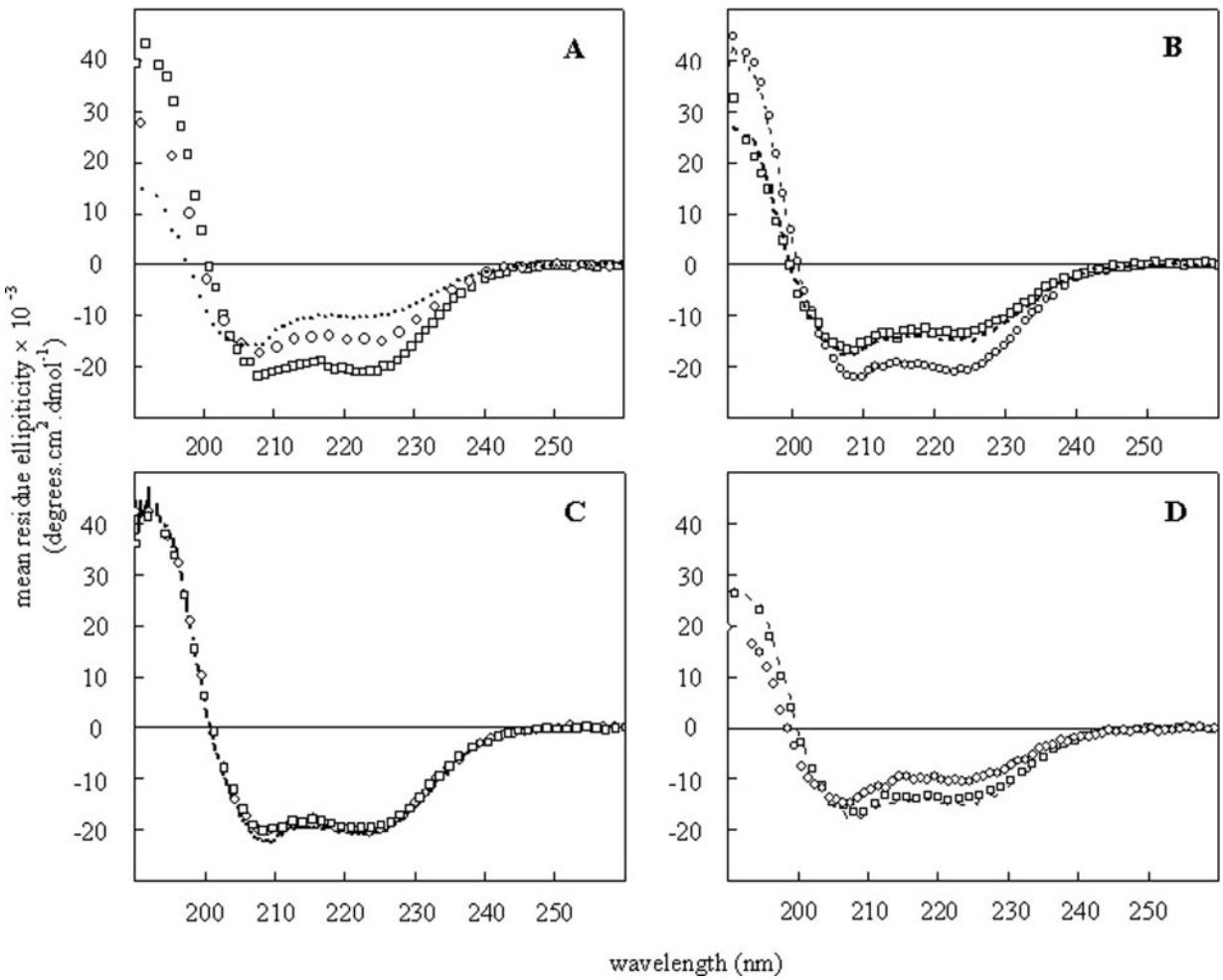

FIG. 3. **CD spectra of the peptide mixtures of TnI HR and TnT2 fragments.** *A*, spectra of peptide mixtures of TnT HR/TnI HR (○) and TnT2/TnI HR (□). The sum of the individual spectra of TnI HR and TnT HR is indicated by the *dotted line*. *B*, spectra of peptide mixtures of TnT-(158–241)/TnI HR (○) and TnT-(179–258)/TnI HR (□). TnT2/TnI HR and TnT HR/TnI HR peptide mixture spectra are shown by *thin* and *thick dotted lines*, respectively. *C*, spectra of peptide mixtures of TnT-(165–241)/TnI HR (○) and TnT-(172–241)/TnI HR (□). The *dotted line* indicates the spectrum of the TnT-(158–241)/TnI HR peptide mixture. *D*, spectra of the TnT-(165–234)/TnI HR (□) and TnT-(165–227)/TnI HR (○). The TnT HR/TnI HR spectrum is shown by the *dotted line*. Spectra were recorded in 10 mM Tris-Cl, pH 7.5, 300 mM NaF, and 1 mM dithiothreitol buffer at 5 °C. Peptide concentrations were 7.5 μM for the dimer.

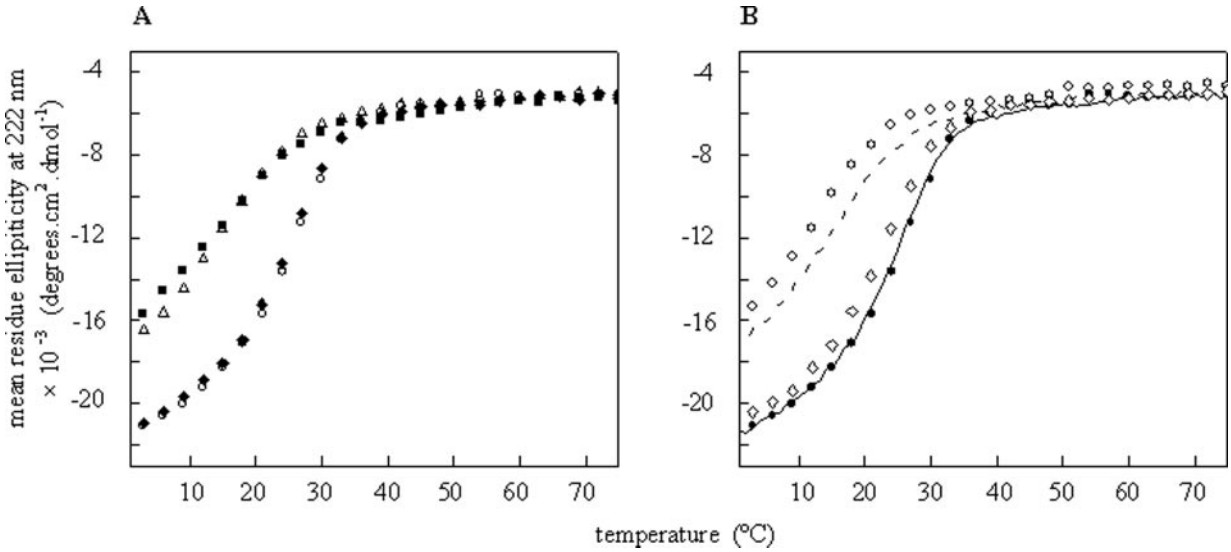

FIG. 4. **Thermal denaturation of the peptide mixtures.** *A*, thermal denaturation spectra of the TnT HR/TnI HR (△), TnT2/TnI HR (♦), TnT-(158–241)/TnI HR (○), and TnT-(179–258)/TnI HR (■). *B*, thermal denaturation spectra of the TnT-(165–241)/TnI HR (●), TnT-(172–241)/TnI HR (◇), and TnT-(165–234)/TnI HR (○). *Dashed* and *solid lines* indicate the denaturation profile of TnT HR/TnI HR and TnT-(158–241)/TnI HR peptide mixtures, respectively. Denaturation was monitored at 222 nm between 0 and 75 °C at a rate of 2 °C/min. Peptide concentrations were 7.5 μM for the dimer, and samples were in 10 mM Tris-Cl, pH 7.5, 300 mM NaF, and 1 mM dithiothreitol buffer.

association states of the peptides at concentrations used in the CD study as well as at high concentrations used for the ITC study (see "Calorimetric Studies of the Interaction of TnI HR with Different TnT2 Fragments"). Sedimentation equilibrium experiments were done with TnI HR, TnT2, TnT-(165–241), TnT-(172–241), and TnT-(165–234) peptides. Experiments were carried out at 5 °C for two sample concentrations of TnT2, TnT-(165–241), and TnT-(165–234) (90 and 30 μM); three concentrations of TnT-(172–241) (90, 30, and 10 μM); and one sample concentration of TnI HR (30 μM). Data from different concentrations of each sample were analyzed together to give a global fit. Fig. 5 shows typical plots of varying concentration of the peptides against the square of radial distance for TnT2, TnT-(165–234), and TnT-(165–234) (Fig. 5, *A*, *B*, and *C*, respectively). Also typical plots of distribution of the residuals from the fitted curve are shown at the *bottom*. Sedimentation data for all the peptides fit nicely to a homogeneous monomer species model (Table II). Using the yeast two-hybrid assay, we have previously reported that the HR domains of both TnT and TnI could form low levels of homodimer as shown by the reporter gene expression assay (18). Our sedimentation equilibrium data indicates that even in high concentration of these peptides, multimeric species were absent.

Having established that the recombinant peptides are monomeric in solution, we next examined their state of association in the complex to determine whether they form heterodimers or other orders of multimers. Sedimentation equilibrium experiments were done for the peptide mixtures of TnI HR with each of TnT2, TnT-(165–241), TnT-(172–241), and TnT-(165–234). Peptide mixtures of TnI HR with TnT2, TnT-(165–241), and TnT-(165–234) were studied in two concentrations (30 and 10 μM) and the mixture of TnI HR and TnT-(172–241) was studied in three concentrations (45, 25, and 10 μM). As above, data from different sets of experiments for each of the peptide mixtures were analyzed together to give a global fit. Fig. 6, *A* and *B*, shows the plots for the TnT2/TnI HR and TnT-(165–241)/TnI HR peptide mixtures, respectively. Data from the each experiment fit well for a two-species monomer-heterodimer association model. This confirmed that when TnT2 fragments were mixed in equimolar amounts with TnI HR, they formed only heterodimers. Details of the sedimentation equilibrium experiments are summarized in Table II.

Calorimetric Studies of the Interaction of TnI HR with Different TnT2 Fragments—ITC was used to determine the association constants and thermodynamically further characterize the interaction of TnI HR with different TnT2 fragments. Fig. 7*A* displays the typical data for the titration of TnI HR with the TnT2 fragment at 5 °C. Heat was released upon addition of TnT2, indicating that the binding of TnI HR to TnT2 was exothermic. Analysis of the binding isotherm yielded a best fit to a single binding site model (Fig. 7*A*, *lower half*) with a K_A value of $1.6 \pm 0.3 \times 10^6$ M^{-1}. Binding was driven by a relatively large negative enthalpy change (-23 ± 1 kcal·mol^{-1}) and was opposed by an unfavorable entropy change (-51 ± 3 cal·mol^{-1}·K^{-1}). Titration of TnI HR with TnT2 performed at 30 °C was not successful and failed to yield a binding isotherm. As evident from the temperature denaturation study of the TnI HR/TnT2 mixture (see "Secondary Structural Analysis by Circular Dichroism Spectroscopy"), the midpoint of the thermal transition was 24 °C, which explains why TnI HR and TnT2 failed to interact at 30 °C. For this reason, the temperature was kept at 5 °C for all the binding experiments. In contrast to the TnT2/TnI HR interaction, TnT HR interaction with TnI HR was significantly weak (Fig. 7*B*) with a 10-fold lower K_A value ($0.1–0.2 \times 10^6$ M^{-1}) as expected from our CD studies data.

Titration of TnT-(158–241) with TnI HR indicated that TnT-(158–241) binds TnI HR with the same affinity as TnT2 as evident from the K_A value of $1.6 \pm 0.1 \times 10^6$ M^{-1} (Table III), whereas the K_A value was only $0.1–0.2 \times 10^6$ M^{-1} for the TnT-(179–258)/TnI HR interaction. This confirmed our CD spectroscopy data that amino acid residues 241–258 C-terminal to the HR region were not able to strengthen the interaction with TnI HR. The enthalpy value for the TnT-(158–241)/TnI HR binding was much higher than that for the TnT-(179–258)/TnI HR binding (Table III), suggesting that TnT-(179–258) lacked a significant amount of binding surface. On the other hand, similar enthalpy and affinity constant values of the TnT-(158–241)/TnI HR and TnT2/TnI HR interactions indicated that the N-terminal residues were involved in the interaction.

The affinity constant for the TnT-(165–241)/TnI HR titration was very similar to those of TnI HR with TnT2 and TnT-(158–241) ($1.3 \pm 0.2 \times 10^6$ M^{-1}), and the enthalpy value was even higher (-29 ± 1 kcal·mol^{-1}), whereas in the case of the TnT-

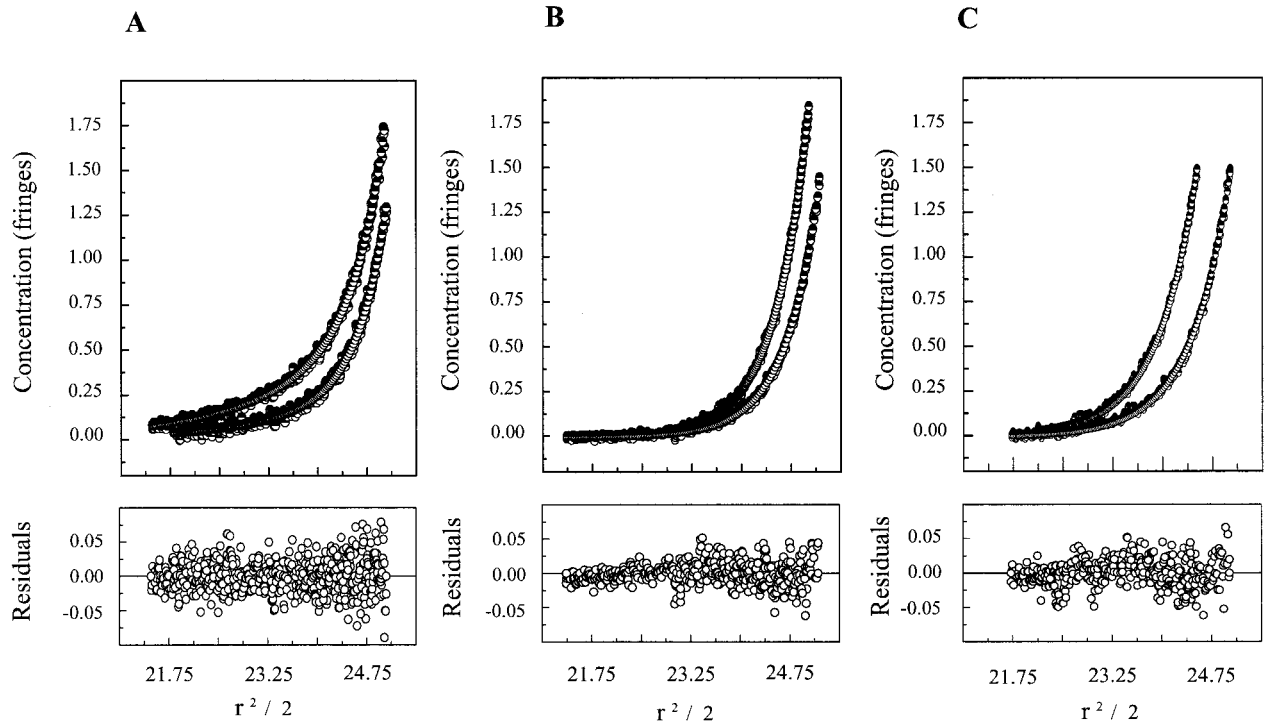

FIG. 5. **Sedimentation equilibrium analysis of the individual peptides.** *A*, TnT2 peptide; *B*, TnT-(165–241) peptide; *C*, TnT-(165–234) peptide. Analyses were done at two concentrations, 90 and 30 μM, for each peptide. The run was performed at 5 °C, and the samples were in a 10 mM Tris-Cl, pH 7.5, 300 mM NaCl, and 1 mM βME buffer. Sedimentation runs were at 36,000 rpm for TnT2 and 40,000 rpm for TnT-(165–241) and TnT-(165–234). Data were fitted for a monodisperse model.

TABLE II
Oligomerization states of the peptides and their mixtures

Species name	Molecular weight[a]	Speed	v^b	σ^c (calculated)	State
		rpm			
TnI HR	7,077	36,000	0.7362	1.110	Monomer
TnT2	14,239	36,000	0.7294	2.295	Monomer
TnT-(165–241)	9,767	40,000	0.7332	1.915	Monomer
TnT-(172–241)	8,997	50,000, 35,000, 25,000	0.7407	2.675, 1.310, 0.668	Monomer
TnT-(165–234)	8,946	40,000	0.7352	1.740	Monomer
TnT2 / TnI HR	21,316	36,000	0.7316	3.406	Heterodimer
TnT-(165–241)/TnI HR	16,844	40,000	0.7344	3.286	Heterodimer
TnT-(172–241)/TnI HR	16,074	50,000, 35,000, 25,000	0.7387	3.083, 1.510, 0.770	Heterodimer
TnT-(165–234)/TnI HR	16,023	40,000	0.7362	3.104	Heterodimer

[a] Molecular weights of the peptides were determined from their amino acid sequences.
[b] The partial specific volumes of the peptides was calculated based on the sequences of the peptides using the SEDNTERP program.
[c] The reduced molecular weight was calculated using the known molecular weights and using the equation $\sigma = M(1-\upsilon\rho)\omega^2/RT$ where υ is the partial specific volume, ρ is the solution density, R is the universal gas constant, T is the temperature in Kelvin, and ω is the angular velocity. The data were fitted with several different models including one species, monomer-dimer, and heterodimer (*i.e.* A + B = C). The best fitting model is indicated in the last column.

(172–241)/TnI HR titration, the K_A value was $1.0 \pm 0.3 \times 10^6$ M^{-1}, and there was a significant decrease in the enthalpy value (-20 ± 1 kcal·mol^{-1}) (Table III), suggesting that the deletion of amino acid residues 165–171 decreased the interacting surface of the TnT2 fragment considerably. The K_A value of the TnT-(165–234) titration with TnI HR ($0.1–0.3 \times 10^6$ M^{-1}) indicated that the amino acid residues 234–241, inside the HR region, were required for optimum binding with TnI HR, although the relatively high enthalpy value (-31 ± 14 kcal·mol^{-1}) suggested that deletion of amino acid residues 234–241 did not affect the interacting surface severely as long as the N-terminal amino acid residues 165–178 were present.

DISCUSSION

We have previously shown that mutations in the HR domain of fsTnT lead to a lack of or a strong decrease in interaction with TnI HR (18), suggesting that the HR domains are involved in a coiled-coil formation. This prediction is consistent with the recently reported crystal structure of the human cardiac Tn core domain that shows the presence of a coiled-coil structure involving a 46-amino acid sequence of the HR domains of cTnT and cTnI (21). Since structural information is still limited for the fast skeletal isoform, we used recombinant fragments of fsTnT and fsTnI to determine the minimal sequence of TnT required for the formation of a stable coiled-coil with TnI HR.

Our CD spectroscopic data indicated that TnT2 and its deletion fragments as well as TnI HR are helical, but the amount of α helicity they contain are quite low, and their secondary structures are dominated by the presence of other elements (Table I). In contrast, equimolar mixtures of different TnT2 fragments and TnI HR showed considerable increase in α helical content indicating a stabilization of the secondary structure when the fragments interact with each other as would be expected in the case of a coiled-coil interaction. Sedimentation equilibrium studies indicated that mixtures of TnI HR and

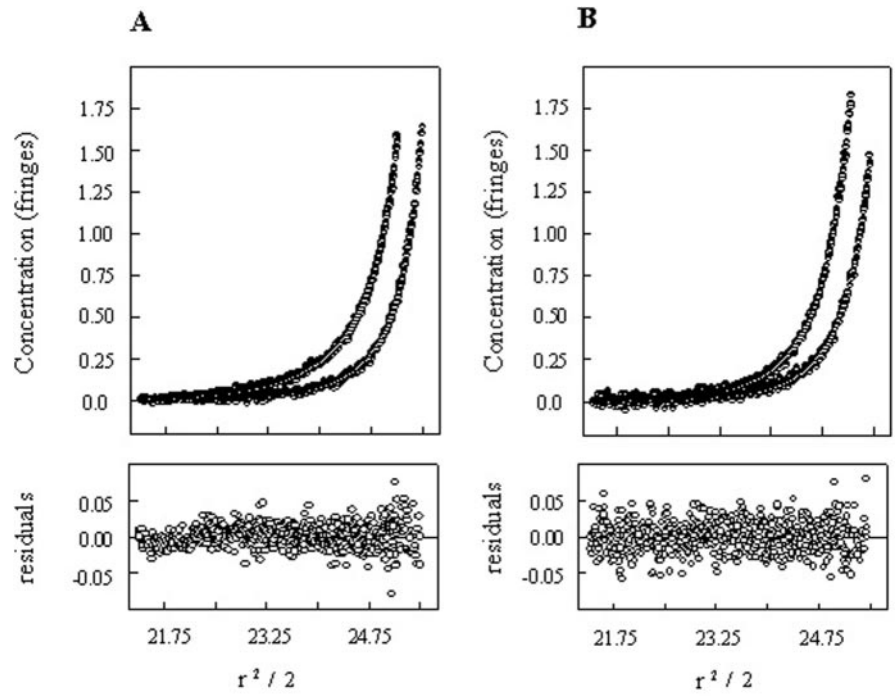

FIG. 6. **Sedimentation equilibrium analysis of the peptide mixtures.** *A*, TnT2/TnI HR peptide mixture; *B*, TnT-(165–241)/TnI HR peptide mixture. Analyses were done at two concentrations, 30 and 10 μM, for each peptide mixture. The run was performed at 5 °C, and the samples were in a 10 mM Tris-Cl, pH 7.5, 300 mM NaCl, and 1 mM βME buffer. Sedimentation runs were at 36,000 rpm for the TnT2/TnI HR peptide mixture and 40,000 rpm for the TnT-(165–241)/TnI HR peptide mixture.

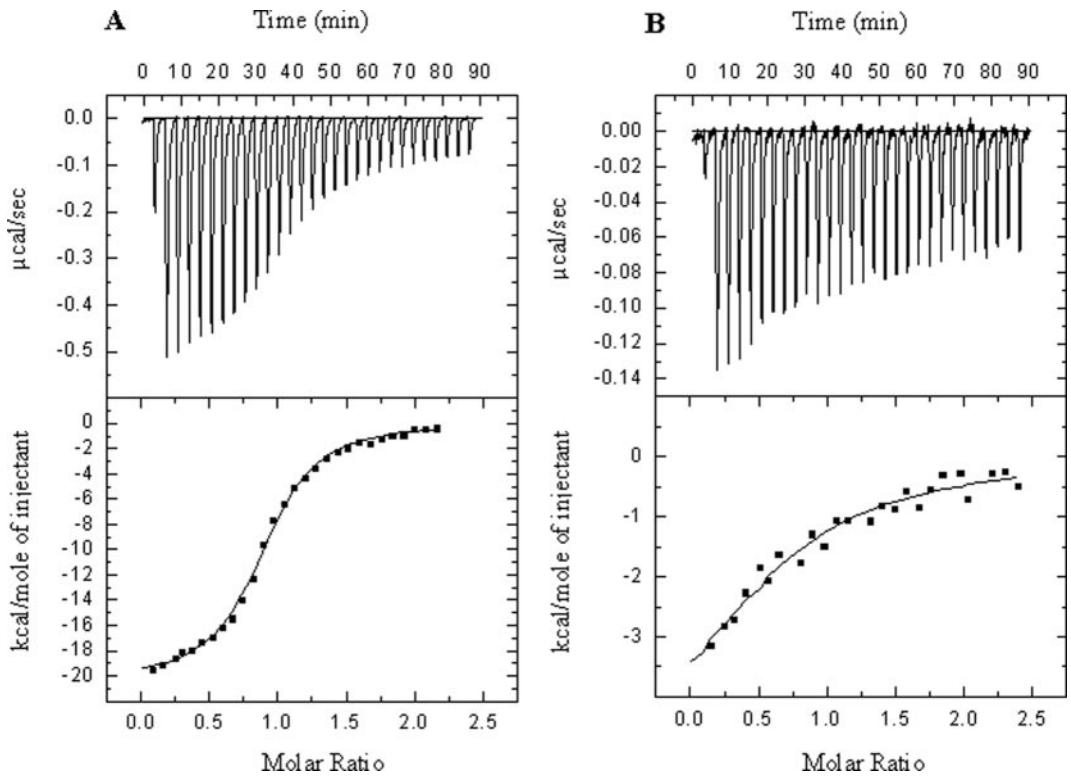

FIG. 7. **Isothermal calorimetric titration of TnT2 fragments with TnI HR.** *A*, titration of TnT2 with TnI HR; *B*, titration of TnT HR with TnI HR. Protein concentrations were 100 μM for TnT2 and TnT HR and 10 μM for TnI HR, and samples were in a 10 mM Tris-Cl, pH 7.5, 300 mM NaCl, and 1 mM βME buffer. Titrations were carried out at 5 °C. For results of all the binding titrations performed, see Table III.

different TnT2 fragments formed heterodimers, whereas single components were all monomeric. We conclude from these observations that TnI HR and TnT2 fragments interacted with each other through the formation of a heterodimeric α helical coiled-coil. However, all the TnT2 fragments did not interact with TnI HR to the same extent. The presence of amino acid residues 165–178 in the TnT2 fragments was required for the formation and stability of the coiled-coil. Thus, only TnT2 (TnT residues 158–258), TnT-(158–241), TnT-(165–241), and TnT-(172–241) formed stable coiled-coil with TnI HR. This is also supported by our ITC data that the K_A value for the interaction with TnI HR was 10 times higher for the TnT2 fragments containing the residues 165–178 than the fragments lacking them (Table III). The temperature denaturation data indicate that the stability of the coiled-coil formed by TnT-(165–241) was slightly higher than the coiled-coil formed by TnT-(172–241), suggesting that the presence of residues 165–171 gave additional stability to the coiled-coil interaction. On the other

TABLE III
Thermodynamic parameters of the binding of TnI HR with different TnT fragments determined by ITC at 5 °C
Thermodynamic parameters reported here are the average of at least two independent experiments with the range of their values indicated.

TnT fragment name	K_A[a]	ΔH[b]	ΔS[c]
	$\times 10^6\ M^{-1}$	$kcal \cdot mol^{-1}$	$cal \cdot mol^{-1} \cdot K^{-1}$
TnT2	1.6 ± 0.3	−23 ± 1	−51 ± 3
TnT HR	0.1 to 0.2[d]	−5 ± 3[e]	−9 ± 4
TnT-(158–241)	1.6 ± 0.1	−21 ± 1	−46 ± 4
TnT-(179–258)	0.1 to 0.2[d]	−13 ± 2[e]	−23 ± 7
TnT-(165–241)	1.3 ± 0.2	−29 ± 1	−77 ± 2
TnT-(172–241)	1.0 ± 0.3	−20 ± 1	−43 ± 4
TnT-(165–234)	0.1–0.3[d]	−15 ± 4[e]	−31 ± 14

[a] Association constant determined by ITC.
[b] Apparent enthalpy change.
[c] Apparent entropy change.
[d] For interactions that were weak in nature, the association constant values are reported as a range, whereas for strong interactions for which the association constant values are obtained with greater precision are reported as average.
[e] For weak interactions the Δ*H* values are less precisely determined compared with the strong interactions.

hand, TnT residues 242–258 appeared to have no stabilizing effect on the heterodimeric interaction as the coiled-coil formed by TnT-(179–258) and TnT HR exhibited the same characteristics.

Analysis of the recently published crystal structure of the cardiac Tn core domain (21) containing cTnC (residues 1–161), cTnI (residues 31–163), and the C-terminal fragment of cTnT (residues 183–288) raises several questions regarding the linkage of the globular core domain of Tn to Tm through TnT1. TnT1 (residues 1–188 for cTnT and residues 1–158 for fsTnT) is believed to have an extended α helical rodlike structure, which binds with Tm through mainly hydrophobic interactions. Residues 158–193, located between the TnT-TnI heterodimeric coiled-coil and the TnT1 region, bridges the TnT1-Tm domain to the core domain. The relative three-dimensional orientation of this region with the rest of the TnT molecule was not well defined in the crystal structure. According to this report, residues 204–220 of cTnT, immediately preceding the coiled-coil domain, form an α helix that is kinked at a 60° angle relative to the coiled-coil. It is anticipated that the corresponding amino acid residues 171–190 in fsTnT would be in the same conformation as that of the cardiac isoform. Our results show that residues 165–178 of fsTnT are required for formation of a stable coiled-coil with TnI HR, although this region is located further upstream from the coiled-coil region. A possible explanation of our observation is that this region (amino acid residues 165–190) is actually closer to the coiled-coil domain than is observed in the crystal structure and thus stabilizes the coiled-coil structure by directly interacting with it.

We have previously shown that a monocysteine mutant TnT ($fsTnT_{S155C}$) cross-links with TnI when 4-maleimidobenzophenone was attached to Cys-155 (14). The binary cross-linking was low in the absence of Ca^{2+} and increased significantly in the ternary complex in the presence of Ca^{2+} suggesting that the region around amino acid residue 155 was sufficiently close to TnI to allow the formation of a cross-linked product. Other studies on the TnT-TnI interaction using CNBr fragments also suggested that fragments that contain residues 158–176 show stronger interaction with TnI than fragments that lack them (32, 33). Furthermore analysis of the TnT HR sequence by coiled-coil prediction algorithms such as pair-coil or multicoil indicates that the fsTnT sequence shows a decreased probability of coiled-coil formation compared with cTnT (18). Accordingly the cardiac TnT-TnI coiled-coil might be inherently stable, whereas for fsTnT other regions (or factors) could be required to stabilize the coiled-coil interaction. Comparative studies using the coiled-coil domains of cardiac and fast skeletal isoforms should answer this question. Taken together, these reports further support our conclusion that the region of fsTnT

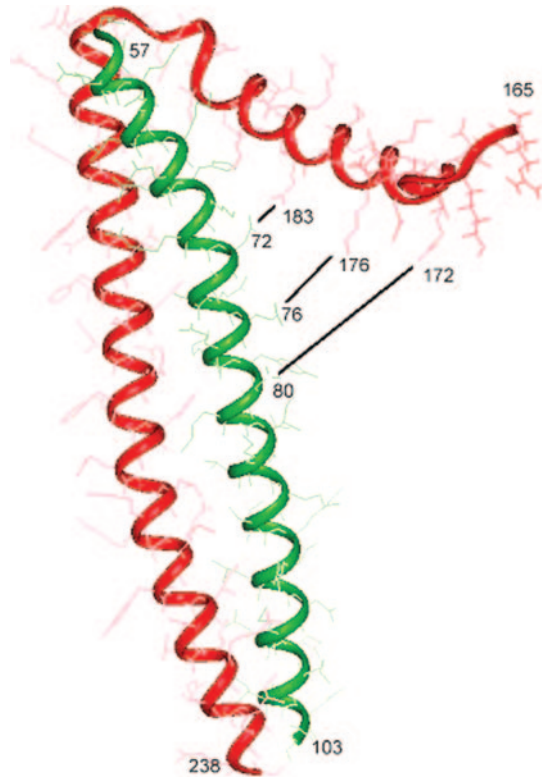

FIG. 8. **A model for the HR region of the fast skeletal TnT/TnI heterodimer.** The model was created from the x-ray crystal structure of the cardiac troponin complex (21). The fsTnT sequence (residues 165–238) is rendered in *red*, whereas the fsTnI sequence (residues 57–103) is in *green*. Hydrogen bond analysis identified a bond between arginine 183 of fsTnT and aspartate 72 of fsTnI. Favorable electrostatic interactions are also observed between lysine 176 of fsTnT and glutamate 76 of TnI and between arginine 172 of fsTnT and aspartate 80 of fsTnI.

containing residues 165–178 plays an important role in the stability of the TnT-TnI interaction.

Based on the available data in the literature regarding the conformation of the region of fsTnT between amino acid residues 165 and 178 and in the light of the recent crystal structure of the Tn core domain of the cardiac isoform, we propose a model (Fig. 8) showing the possible conformation of this region relative to the coiled-coil structure in the fast skeletal TnT-TnI complex. Interaction of the TnT fragment between residues 165 and 178 and the fragment of TnT or TnI participating in the coiled-coil structure could stabilize the coiled-coil presumably through ionic interactions. The TnT 165–178 region most likely

interacts with the proximal amino acid residues of the TnI HR fragment. Indeed the modeling shows two amino acid residues, arginine 172 and lysine 176, of TnT can participate in electrostatic interactions with residues aspartate 80 and glutamate 76, respectively, located on the TnI HR fragment (Fig. 8). Interestingly the fsTnT contains a proline residue at position 185 that is not present in the cTnT, and this could significantly lead to differences in the conformation of the region 165–178 between cardiac and fast skeletal isoforms. Taken together with the fact that a large number of charged amino acid residues are present throughout the region 165–178, this also raises the possibility of additional electrostatic interactions.

The cardiac crystal structure shows the length of the cTnT fragment involved in the coiled-coil interaction as 46 residues (21). It is anticipated that for the skeletal Tn isoform the length of the TnT involved in the coiled-coil structure would be the same. Our results showed that deletion of heptads at the C-terminal end of the HR region (TnT-(165–234) and TnT-(165–227)) dramatically decreases the coiled-coil stability. This suggests that the C-terminal ends of the coiled-coil are the same for both cardiac and fast skeletal isoforms as residue 241 in fsTnT corresponds to residue 271 of the cTnT. Thus, the 14 amino acid residues (179–192) located at the N terminus of the conserved HR region of fsTnT together with the residues 165–178 constitute the fragment required for the stabilization of the coiled-coil in the fast skeletal isoform.

In general, stability of coiled-coil structures depends on hydrophobic residues at positions "a" and "d" of the heptad repeats. Hydrophilic residues at other positions augment the stability through ionic interactions (34–36). Our results indicate that the TnT region 165–178 located outside the coiled-coil domain plays a significant role in stabilizing the TnT-TnI coiled-coil structure. This might be a result of either ionic interactions involving residues in the region 165–178 or formation of a partial trimeric structure at the end of the fast skeletal TnT-TnI coiled-coil. An interesting characteristic of this region is the overall conserved nature of the amino acid sequence. Alignment of TnT sequences (residues 165–192) from different species ranging from *Drosophila* to human and between different muscle isoforms (21) reveals seven conserved amino acid residues: lysine 167, glutamine 169, glutamic acid 173, lysine 175, leucine 179, arginine 182, and leucine 186. In contrast, the region of TnT containing the entire coiled-coil region contains only nine completely conserved residues. The high degree of sequence conservation in the 165–192 region is intriguing and suggests that it may be important for the structural integrity of the Tn complex, especially as many of these residues are potential candidates for salt bridge formation. Our model, built using the cardiac coordinates (Fig. 8), also suggests the likelihood of stabilizing ionic interactions; however, the exact positioning of the putative salt bridges is slightly out of register with the conserved amino acid residues, possibly due to conformational differences between the cardiac and fast skeletal isoforms. We are currently trying to refine our model and to assess the importance of the conserved amino acid residues in the fast skeletal isoform by measuring the stability of a series of site-selective mutants.

REFERENCES

1. Gordon, A. M., Homsher, E., and Regnier, M. (2000) *Physiol. Rev.* **80,** 853–924
2. Ebashi, S., Endo, M., and Otsuki, J. (1969) *Q. Rev. Biophys.* **2,** 351–384
3. Phillips, G. N., Jr., Fillers, J. P., and Cohen, C. (1986) *J. Mol. Biol.* **192,** 111–131
4. Farah, C. S., and Reinach, F. C. (1995) *FASEB J.* **9,** 755–767
5. Leavis, P. C., and Gergely, J. (1984) *CRC Crit. Rev. Biochem.* **16,** 235–305
6. Zot, A. S., and Potter, J. D. (1987) *Annu. Rev. Biophys. Biophys. Chem.* **16,** 535–539
7. Perry, S. V. (1998) *J. Muscle Res. Cell Motil.* **19,** 575–602
8. Schaertl, S., Lehrer, S. S., and Geeves, M. A. (1995) *Biochemistry* **34,** 15890–15894
9. Lehrer, S. S., and Geeves, M. A. (1998) *J. Mol. Biol.* **277,** 1081–1089
10. Geeves, M. A., and Lehrer, S. S. (1994) *Biophys. J.* **67,** 273–282
11. Potter, J. D., Zheng, Z., Pan, B. S., and Zhao, J. (1995) *J. Biol. Chem.* **270,** 2557–2562
12. Malnic, B., Farah, C. S., and Reinach, F. C. (1998) *J. Biol. Chem.* **273,** 10594–10601
13. Jha, P. K., Leavis, P. C., and Sarkar, S. (1996) *Biochemistry* **35,** 16573–16580
14. Jha, P. K., and Sarkar, S. (1998) *Biochemistry* **37,** 12253–12260
15. Oliveira, D. M., Nakaie, C. R., Sousa, A. D., Farah, C. S., and Reinach, F. C. (2000) *J. Biol. Chem.* **275,** 27513–27519
16. Stefancsik, R., Randall, J. D., Mao, C. J., and Sarkar, S. (2003) *Comp. Funct. Genom.* **4,** 609–625
17. Blumenschein, T. M., Tripet, B. P., Hodges, R. S., and Sykes, B. D. (2001) *J. Biol. Chem.* **276,** 36606–36612
18. Stefancsik, R., Jha, P. K., and Sarkar, S. (1998) *Proc. Natl. Acad. Sci. U. S. A.* **95,** 957–962
19. Pearlstone, J. R., and Smillie, L. B. (1985) *Can. J. Biochem.* **63,** 212–218
20. Perry, S. V. (1999) *Mol. Cell. Biochem.* **190,** 9–32
21. Takeda, S., Yamashita, A., Maeda, K., and Maeda, Y. (2003) *Nature* **424,** 35–41
22. Wu, Q. L., Jha, P. K., Raychowdhury, M. K., Du, Y., Leavis, P. C., and Sarkar, S. (1994) *DNA Cell Biol.* **13,** 217–233
23. Wu, Q. L., Raychowdhury, M. K., Du, Y., Jha, P. K., Leavis, P. C., and Sarkar, S. (1993) *J. DNA Sequencing Mapping* **4,** 113–121
24. Sreerama, N., and Woody, R. W. (1993) *Anal. Biochem.* **209,** 32–44
25. Cooper, T. M., and Woody, R. W. (1990) *Biopolymers* **30,** 657–676
26. Dutta, K., Alexandrov, A., Huang, H., and Pascal, S. M. (2001) *Protein Sci.* **10,** 2531–2540
27. John, D. M., and Weeks, K. M. (2000) *Protein Sci.* **9,** 1416–1419
28. Stafford, W. F., and Sherwood, P. J. (2004) *Biophys. Chem.* **108,** 231–243
29. Lau, S. Y., Taneja, A. K., and Hodges, R. S. (1984) *J. Biol. Chem.* **259,** 13253–13261
30. Zhou, N. E., Kay, C. M., and Hodges, R. S. (1992) *J. Biol. Chem.* **267,** 2664–2670
31. Steinmetz, M., Stock, A., Schulthess, T., Landwehr, R., Lustig, A., Faix, J., Gerisch, G., Aebi, U., and Kammerer, R. (1998) *EMBO J.* **17,** 1883–1891
32. Chong, C. S., and Hodges, R. S. (1982) *J. Biol. Chem.* **257,** 11667–11672
33. Pearlstone, J. R., and Smillie, L. B. (1980) *Can. J. Biochem.* **56,** 659–664
34. Zhou, N. E., Kay, C. M., and Hodges, R. S. (1994) *Protein Eng.* **7,** 1365–1372
35. Vu, C., Robblee, J., Werner, K. M., and Fairman, R. (2001) *Protein Sci.* **10,** 631–637
36. Meier, M., Lustig, A., Aebi, U., and Burkhard, P. (2002) *J. Struct. Biol.* **137,** 65–72

Identification of a Region of Fast Skeletal Troponin T Required for Stabilization of the Coiled-coil Formation with Troponin I

Subhradip Mukhopadhyay, Knut Langsetmo, Walter F. Stafford III, Gillian D. Henry, James D. Baleja and Satyapriya Sarkar

J. Biol. Chem. 2005, 280:538-547.
doi: 10.1074/jbc.M409537200 originally published online October 26, 2004
